Current Research in Microbial Sciences 1 (2020) 7–17

Contents lists available at ScienceDirect

Current Research in Microbial Sciences

journal homepage: www.elsevier.com/locate/crmicr

In Situ Intraepithelial Localizations of Opportunistic Pathogens, *Porphyromonas gingivalis* and *Filifactor alocis,* in Human Gingiva

Jaden S. Lee[a,1], Ralee Spooner[b,c,1], Nityananda Chowdhury[a], Vivek Pandey[a], Bridgette Wellslager[a], Kalina R. Atanasova[d], Zachary Evans[b], Özlem Yilmaz[a,e,*]

[a] Department of Oral Health Sciences, College of Dental Medicine, Medical University of South Carolina, Charleston, South Carolina, 29425, USA
[b] Department of Stomatology, Division of Periodontics, College of Dental Medicine, Medical University of South Carolina, Charleston, South Carolina, 29425, USA
[c] Lieutenant, Dental Corps, United States Navy, Marine Corps Air Ground Combat Center, Twentynine Palms, California, 92278, USA
[d] Department of Periodontology, University of Florida, Gainesville, Florida, 32611, USA
[e] Department of Microbiology & Immunology, Medical University of South Carolina, Charleston, South Carolina, 29425, USA

ARTICLE INFO

Keywords:
Porphyromonas gingivalis
Filifactor alocis
Periodontal epithelium
Dual species colonization in gingiva
Metabolically active bacteria in human tissue

ABSTRACT

Porphyromonas gingivalis and *Filifactor alocis* are fastidious oral pathogens and etiological agents associated with chronic periodontitis. Although previous studies showed increased levels of the two obligate anaerobic species in periodontitis patients, methodologies for this knowledge were primarily limited to sampling subgingival plaque, saliva, or gingival crevicular fluid. To evaluate the extent to which *P. gingivalis* and *F. alocis* may invade the periodontal tissues, an *in situ* cross-sectional study was comparatively conducted on the gingival biopsy specimens of patients diagnosed with periodontal health or chronic periodontitis. Immunostained tissue sections for each organism were imaged by Super-Resolution Confocal Scanning Microscopy to determine the relative presence and localization of target bacterial species. Fluorescence-in-situ-hybridization (FISH) coupled with species specific 16S rRNA method was utilized to confirm whether detected bacteria were live within the tissue. In periodontitis, *P. gingivalis* and *F. alocis* revealed similarly concentrated localization near the basement membrane or external basal lamina of the gingival epithelium. The presence of both bacteria was significantly increased in periodontitis vs. healthy tissue. However, *P. gingivalis* was still detected to an extent in health tissue, while only minimal levels of *F. alocis* were spotted in health. Additionally, the micrographic analyses displayed heightened formation of epithelial microvasculature containing significantly co-localized and metabolically active dual species within periodontitis tissue. Thus, this study demonstrates, for the first-time, spatial arrangements of *P. gingivalis* and *F. alocis* in both single and co-localized forms within the complex fabric of human gingiva during health and disease. It also exhibits critical visualizations of co-invaded microvascularized epithelial layer of the tissue by metabolically active *P. gingivalis* and *F. alocis* from patients with severe periodontitis. These findings collectively uncover novel visual evidence of a potential starting point for systemic spread of opportunistic bacteria during their chronic colonization in gingival epithelium.

Introduction

Chronic periodontitis is a prevalent inflammatory condition of the oral cavity with strong polymicrobial etiology posing a significant public health burden. Furthermore, the disease's comorbidity with multiple chronic conditions have lately been highlighted (Pihlstrom et al., 2005). Studies on the microbial etiology of periodontitis have demonstrated highly diverse and thriving state of the oral microbial and bacterial communities sparking long lasting fascination for understanding the complex bacterial interactions in disease versus health (Socransky and Haffajee, 2005, Socransky and Haffajee, 1992, Saglie et al., 1982, Lamont et al., 2018, Hajishengallis et al., 2012). The proliferation of advanced molecular, morphological, and structural studies on the oral microbes within the last two decades have culminated in the inception of multiple novel paradigms for the pathobiology of periodontitis with several specific subsets of bacterial complexes being repeatedly found together in the pathogenic biofilms and historically categorized, such as the "red complex" bacteria (*i.e., Porphyromonas gingivalis*, *Tannerella forsythia*, and *Treponema denticola*) (Socransky et al., 1998). More recently, *Filifactor alocis* was identified as one of the most abundant bacterial organisms in deep periodontal pockets of subjects with the severe chronic forms of periodontitis (Aruni et al., 2011). *P. gingivalis* and *F. alocis* are recognized as centrally significant contributing factors for chronic periodontal inflammation, due to being fastidious anaerobes with immune evasion capabilities, while their biology and pathogenic properties may differ (Aruni et al., 2011, Dewhirst et al., 2010). In our

* Corresponding author.
E-mail address: yilmaz@musc.edu (Ö. Yilmaz).
[1] J.S.L. and R.S contributed equally to this work.

https://doi.org/10.1016/j.crmicr.2020.05.001
Received 23 March 2020; Received in revised form 30 April 2020; Accepted 1 May 2020

earlier study, we assessed bacterial growth activity and abundance of *P. gingivalis* and *F. alocis* in periodontitis patients' subgingival plaques before and after non-surgical periodontal therapy (Spooner et al., 2016) and found decreased prevalence of actively growing *P. gingivalis* post-therapy, which is consistent with existing literature (Colombo et al., 2012, Colombo et al., 2009, Junemann et al., 2012). Interestingly, there was no significant reduction of actively growing *F. alocis* post-therapy, whereas gDNA level quantification showed significantly decreased total load of both species in abundance (Spooner et al., 2016).

In periodontitis patients, both *P. gingivalis* and *F. alocis* are shown to be present in high abundance compared to those with healthy periodontium (Spooner et al., 2016, Yang et al., 2004, Kumar et al., 2006). Conventional periodontal treatment often fails to decrease the presence of pathogens such as *P. gingivalis* and *F. alocis* which could be due to their abilities to adapt to the epithelial cellular environment and invade deeper tissues (Spooner et al., 2016, Ji et al., 2015). While no prior studies of *F. alocis* in the context of tissue invasion in the human gingiva exist, multiple former studies conducted on human gingival samples (Colombo et al., 2007, Baek et al., 2018, Rajakaruna et al., 2018, Katz et al., 2011); and system level characterizations in human primary gingival epithelial cells (Yilmaz et al., 2006, Yilmaz, 2008, Lee et al., 2017, Lee et al., 2018, Lee et al., 2018) undoubtedly depict *P. gingivalis'* chronic intra- and trans-cellular presence in gingival epithelium and in deeper tissue. Given the described *F. alocis* centered polymicrobial group formation in periodontitis patients (Chen et al., 2015) and the proposed synergy between *P. gingivalis* and *F. alocis* (Spooner et al., 2016) from patient subgingival plaques, these two bacteria may also establish dual-colonization niches inside gingival epithelia to synergistically build a covert way and a reservoir against host immune defenses.

Since existing studies demonstrating the localization of periodontal pathogens within the human gingiva remain limited, it is timely to understand the tissue spatial distributions and viability status of these opportunistic pathogens in gingival health versus periodontal disease through robust methods. Periodontitis increases the risk of bacteremia caused by normal oral function and dental procedures (Bale et al., 2017). In the absence of periodontal disturbance, the vascular system usually remains sterile, which can be attributed to the oral mucosal epithelium serving as a physical barrier with a variety of antibacterial host defense machineries (Lee et al., 2017, Lee et al., 2018, Roberts et al., 2017, Atanasova et al., 2016, Bui et al., 2016, Spooner et al., 2014, Hung et al., 2013, Yilmaz et al., 2004). The dental bacteremia is rapidly gaining attention due to the increasingly observed correlations between periodontal pathogens and systemic diseases such as orodigestive cancers and Alzheimer's disease (Olsen and Yilmaz, 2019, Atanasova and Yilmaz, 2015, Atanasova and Yilmaz, 2014, Dominy et al., 2019). Systemic dissemination of periodontal pathogens and their potential contribution to systemic diseases has primarily been evaluated in experimental animal models. However, there is a lack of patient data that substantiate these hypotheses, and a lack of understanding how these pathogens spatially exist and interact with the host tissues in setting of health and disease. This includes to what extent they colocalize within tissue, and to what tissue structures these pathogens invade and penetrate.

Thus, in this study, we utilized gingival tissue biopsies from patients in periodontal health and periodontitis with advanced microscopy to visualize intratissue colonization of *P. gingivalis* and *F. alocis* in conjunction with examining their spatial arrangement, abundance, viability and localization.

Material and methods

Study design, human subject population and gingival biopsy specimen collection

The human study protocol and written consent form were approved by the Medical University of South Carolina, Institutional Review Board under the human subjects assurance number, FWA00001888 (with all applicable federal regulations governing the protection of human subjects). Briefly, patients in the MUSC Graduate Periodontics clinic were given an oral examination as part of their routine care and the periodontal status/diagnosis were determined based on the guidelines of the American Academy of Periodontology (American Academy of Periodontology Task Force 2015). Following oral examination and obtaining signed consent, participants treatment planned for dental implant placement in an edentulous space at future surgical appointment(s) were designated in "healthy group" and their soft tissue attached to an adjacent tooth in edentulous space was selected for specimen collection. In the same manner, participants diagnosed with chronic periodontitis and scheduled for future periodontal surgical therapy were selected as "periodontitis" group upon obtaining signed consent. Specimens collected from healthy individuals and chronic periodontitis patients were processed further as described below. In periodontitis group, the worst probing depths in each quadrant were selected for specimen collection. With local anesthesia, whole gingival specimens containing pericoronal/radicular epithelium and subepithelial connective tissue were excised and immersed in 20% neutral buffered formalin. On average, a collar of tissue collected from each patient had an estimated volume of 20-60 mm^3. After fixation, the tissue specimens were embedded in paraffin and sectioned. Cuts of specimens were stained with hematoxylin and eosin (H&E) for gross viewing of tissue. Detailed information regarding patient population demographics, exclusion /inclusion criteria, age, body mass index (BMI) and clinical parameters including periodontal pocket depth (PPD), clinical attachment level (CAL), bleeding on probing (BOP), and plaque index are summarized in Table 1.

Bacterial and human primary gingival epithelial cell control experiments for further validity of bacterial antibodies

The *P. gingivalis* ATCC strain 33277 was cultured under anaerobic conditions in Trypticase soy broth (TSB) supplemented with yeast extract (1 μg/ml), menadione (1 μg/ml), and hemin (5 μg/ml), at 37°C and harvested as described previously (Lee et al., 2017, Roberts et al., 2017, Choi et al., 2013). The number of bacteria for infection was determined at mid-log phase using a Klett-Summerson photometer and used at a multiplicity of infection (MOI) of 100. *F. alocis* ATCC 35896 was cultured as described previously (Spooner et al., 2016) in anaerobic conditions for 36 h at 37 °C in brain heart infusion (BHI) (Fisher Scientific, Pittsburg, PA) supplemented with yeast extract (0.5 mg/mL) (Fisher Scientific, Pittsburg, PA), L-cysteine (50 μg/mL) (Sigma-Aldrich, St. Louis, MO), and 20% arginine (Fisher Scientific, Pittsburg, PA). All the experiments were performed in our Biosafety Level 2 laboratory approved by the institutional biosafety committee.

Primary human gingival epithelial cells (GECs) were obtained from adult patients who were selected randomly and anonymously from those presenting for tooth crown lengthening or impacted third molar extraction. Gingival tissue was collected under the approved guidance of the University of Florida Health Science Center Institutional Review Board (IRB, human subjects assurance number FWA 00005790). No patient information was collected, and the informed consent was obtained by all subjects. Cells were cultured in serum-free keratinocyte growth medium (KGM, Lonza, Walkersville, MD) at 37°C in 5% CO2 as previously described (Lamont et al., 1995, Yilmaz et al., 2008, Yilmaz et al., 2003).

Immunostaining for P. gingivalis, F. alocis*, and CD31*

The tissue sections from healthy individuals and periodontitis patients were deparaffinized according to the following protocol. Sections were heated for 30min at 60°C and immediately immersed in 100% xylene (Fisher Scientific, Pittsburg, PA) for 7min. Following 20 washes in a second 100% xylene solution, the specimens were transferred for 20 washes to a 100%, 95%, and 70% ethanol solution before a 5-min wash in PBS. Samples were transferred to a 15mM citrate buffer solution for antigen retrieval and placed into a pressure cooker on the low

Table 1
Detailed patient population profile. (A) Inclusion criteria for "health" and "periodontitis" groups. (B) Clinical parameters including the average periodontal pocket depth (PPD), and clinical attachment level (CAL), bleeding on probing (BOP) (present/absent), and plaque index (present/absent) from patients in health and periodontitis. PPD and CAL were averaged within the group and the significant difference between two groups for each parameter was determined by unpaired two-tailed student T-test (*p < 0.05, ** p < 0.0001). BOP and plaque index were presented in percentages (the number of participants with BOP or plaque / all participants within the group). (C) General population information for health and periodontitis groups. Age and body mass index (BMI) are presented in mean ± SD. M = male, F = female, C = Caucasian, A = African American. (D) A list of exclusion criteria used for the study in accordance with criteria determined by AAP. No exclusion was made based on sex or race.

A

Criteria	Health	Periodontitis
BOP	< 30% of total gingival probing sites with BOP	At least one quadrant
PPD	< 4mm	≥ 5mm
Sub-gingival calculus	Absent	Present

B

Clinical parameter	Health	Periodontitis
PPD (Buccal)	2.20 ± 0.45 mm	6.40 ± 1.14 mm**
PPD (Lingual)	2.40 ± 0.89 mm	8.00 ± 1.22 mm**
CAL (Buccal)	3.80 ± 1.92 mm	7.20 ± 1.30 mm*
CAL (Lingual)	2.20 ± 1.48 mm	8.00 ± 1.22 mm**
BOP	0%	83.3%
Plaque	0%	15.4%

C

Population information	Health	Periodontitis
Total patients	5	7
Age (years)	69.0 ± 5.34	60.0 ± 12.2
Sex	M – 4	M – 0
	F – 1	F – 7
Race	C – 5	C – 6
	A – 0	A – 1
BMI	31.0 ± 6.26	29.7 ± 8.09

D
Exclusion criteria

- Diagnosis with any uncontrolled systemic disease
- Self-reporting smokers
- Pregnant women
- History of taking systemic or local antibiotics within the previous 3 months
- History of receiving scaling and root planing or surgical periodontal therapy within the previous 12 months

setting for 15min. After cooling down the slides in the citrate buffer at room temperature (RT) for 20min, they were air-dried prior to antibody staining. For single species staining, the specimens were incubated with custom-made 1:200 rabbit anti-*P. gingivalis* ATCC 33277 (Lee et al., 2018) or 1:200 rabbit anti-*F. alocis* ATCC 35896 (Pacific Immunology, Ramona, CA) in PBS for 24h overnight at 4°C. Specimens were washed with PBS and secondary antibody staining was completed using 1:500 Alexafluor-488-conjugated goat anti-rabbit in PBS for 1h at RT. 1:500 DAPI was used to stain nuclear material for 5min at RT. Specimens were then washed in PBS at RT for 5min before undergoing dehydration steps. Briefly, the above outlined deparaffinization and hydration steps were reversed, with the final incubation with a fresh xylene solution to avoid paraffin fragments. Slides were air-dried, coverslips were mounted, and imaging was completed the following day. For dual species detection, the rabbit anti-*F. alocis* ATCC 35896 and mouse anti-*P. gingivalis* ATCC 33277 (Bore Da Biotech Co., LTD, South Korea) (Lee et al., 2017) antibodies were incubated and reacted with Alexafluor-568 conjugated goat anti-rabbit and Alexafluor-488-conjugated goat anti-mouse respectively. Control tissue sections without either primary antibodies or secondary antibodies were used in the same manner to further verify the specificity of the antibodies used in this study.

As a counterstaining, a host molecule CD73, which has been recently shown to have robust expression in the gingival epithelium, was used (Lee et al., 2020). The tissue samples were incubated in a 1:50 anti-CD73 mouse monoclonal antibody overnight (Abcam, Cambridge, MA). The tissues were then washed with PBS and incubated in 1:250 Alexafluor-568-conjugated goat anti-mouse secondary antibody for 1h at RT. The subsequent procedure was completed as the immunostaining described above. Control tissue sections without either anti-CD73 primary antibody or the secondary antibody used in the same manner to further verify their specificity.

To confirm the visualization of blood vessels in the gingival epithelium, CD31, a commonly used vascular marker (Yu et al., 2016, Azaripour et al., 2018), was stained using an anti-CD31 mouse monoclonal antibody (Cell Signaling, Danvers, MA). Tissue sections processed as described above were simultaneously incubated with 1:1,000 anti-CD31 mouse antibody and 1:200 rabbit anti-*P. gingivalis* antibody overnight. The slides were then washed with PBS and secondary antibody staining was completed using 1:250 Alexafluor-568-conjugated goat anti-mouse antibody and 1:500 Alexafluor-488-conjugated goat anti-rabbit antibody in PBS for 1h at RT. The subsequent procedure was completed as the immunostaining described above. Control tissue sections without either anti-CD31 primary antibody or the secondary antibody used in the same manner to further verify their specificity.

Detection of metabolically active P. gingivalis *and* F. alocis *by fluorescence in situ hybridization (FISH)*

To determine *P. gingivalis* and *F. alocis* detected within the gingival tissue through specific antibody staining were live bacteria, simultaneous FISH was performed using probes specific to each bacterial 16s rRNA. Tissue sections processing and hybridization with FISH probes were performed as described before with few changes as defined below (Velsko et al., 2014, Schlafer et al., 2010). In brief, tissue sections mounted on microscope glass slides were deparaffinized and blocked with 1% BSA/0.1% Triton-X 100 in PBS at RT for 30min. The slides were washed with distilled water and hybridized with 5nM FISH *P.*g-488 probe (*P. gingivalis* 16S rRNA-specific oligonucleotide POGI (Velsko et al., 2014, Sunde et al., 2003) 5'-CAATACTCGTATCGCCCGTTATTC-3' labeled with Alexafluor-488 (green fluorescent) at the 5'-end) and/or FISH *F.*a-594 probe (F. *alocis* 16S rRNA-specific oligonucleotide FIAL (Schlafer et al., 2010) 5'- TCT TTG TCC ACT ATC GTT TTG A-3' labeled with Alexafluor-594 (red fluorescent) at the 5'-end) (Eurofins Genomics LLC, Louisville, KY) diluted in hybridization buffer (0.9M NaCl, 20mM Tris/HCl, pH 7.3, and 0.01% SDS, 20% formamide) for 4h in dark at 46°C. The slides were washed with distilled water and 1:500 DAPI was used to stain for nuclear material for 5min at RT. Finally, the slides were dehydrated and mounted with nonfluorescent immersion oil and covered with coverslips for visualization.

Imaging of samples and image processing

Gingiva tissue sections were imaged using super resolution confocal scanning microscopy (Zeiss 880 LSM NLO Airyscan; 1024 × 1024 pixels; magnification: 63x unless specified otherwise) and/or fluorescence microscopy (Zeiss Axio Imager A1 with QImaging MicroPublisher 3.3). The fluorescence was measured at an excitation of 488 nm and emission of 526 for green, an excitation of 561 nm and emission of 650 for red, and excitation of 405 nm and emission of 453 for blue (DAPI). For all samples, 20-35 slices of z-stacks were obtained with each slice at 0.4-0.6μm. A mid-slice within each tissue was chosen for analysis and

image presentation. To process data sets, Zeiss Zen imaging software and QCapture Pro software were used for confocal/epifluorescence microscopy, respectively. Representative images were selected to visually display any differences in the antibody staining.

Quantitative analysis of bacterial presence and co-localization within the gingival tissue

Mean fluorescent intensity for individual staining of *P. gingivalis* and *F. alocis* was quantified using NIH Image J software as previously described (Atanasova et al., 2016, Zhang et al., 2020, Choi et al., 2011). Briefly, at least 5 confocal images representing separate regions of interest (ROIs) with the same dimension (225 × 225 μm) within each of subjects' gingival tissue were obtained, while keeping the relative location of ROIs consistent across all images. For each ROI, mean intensity for *P. gingivalis* or *F. alocis* staining was calculated by Image J and all values were averaged within each subject as well as each group. Threshold was set in a way that there are no over- and undersaturated pixels. The averaged intensity value of the healthy group was used for normalization to indicate a fold-increase in periodontitis group. To quantify the degree of co-localization between *P. gingivalis* and *F. alocis* fluorescence within the periodontitis tissue, the Pearson correlation coefficient, a well-established measure of calculating the co-localization between two fluorophores (Dunn et al., 2011), was obtained via NIH Image J software with JACoP plug-in (Bolte and Cordelieres, 2006). At least 5 separate ROIs with the same dimension (225 × 225 μm) were selected within each periodontitis tissue section. The imaging parameters were kept consistent across all samples imaged and used for quantifications. Representative images were selected to visually display any differences in the antibody staining.

Semi-quantitative analysis of gingival microvasculature formation and bacterial presence within the vessels

To determine the number of participants within each group that showed formation of gingival microvasculature as well as the overall abundance of microvessels invaded by the bacteria within the tissue, the whole epithelial layer of the collected gingival tissue in at least 3 different sectioned slides for all healthy individuals and periodontitis patients were screened and the presence or absence of gingival microvasculature was recorded and reported in percentages. Further, all fluorescent images of periodontitis tissues showing gingival microvasculature formation were used to examine the number of microvessels occupied by *P. gingivalis* and *F. alocis* out of the total microvessels detected within each tissue.

Further Verification of P. gingivalis *and* F. alocis *FISH probe specificity* in vitro

To further ensure no cross-activity between the FISH probes, we cultured *P. gingivalis* ATCC 33277 and *F. alocis* ATCC 35896 anaerobically as previously described (Spooner et al., 2016, Roberts et al., 2017, Atanasova et al., 2016, Hung et al., 2013), fixed the bacterial cells on microscopic slides (Corning, NY) using 10% neutral buffered formalin for 15min, and hybridized the bacteria separately in P.g-488 and F.a-594 FISH probes as described above. Coverslips were mounted onto the slides using VectaShield mounting medium containing DAPI (Vector Laboratories, Burlingame, CA). The slides were imaged using epifluorescence microscopy. At least 3 biological replicates were performed for each experiment and representative images were selected to visually display any differences in the observed fluorescent pattern.

Statistical analysis

At least 3 separate tissue sections for each participant's sample were used for all imaging analysis. Quantification of fluorescent intensity is expressed as mean ± SD. Two-tailed Student's t-test was used to calculate the statistical significance of the experimental results between healthy and periodontitis groups (significance considered at $p < 0.05$).

Results

Differential presence and localization of P. gingivalis *in the gingival epithelium in health and periodontitis*

Histology of gingival epithelial tissue from chronic periodontitis patients uniformly showed heightened microvasculature formation and irregulates of the basement membrane compared to healthy individuals (Fig. 1A). Using anti-*P. gingivalis* antibodies (Lee et al., 2017, Lee et al., 2018) with further verified specificity in Fig. 1B, substantially higher levels (~ 3-fold) of *P. gingivalis* were revealed in periodontitis tissue compared to health (Fig. 1C, D). Majority of the detected bacteria were localized within the deeper layers of the epithelium near the basement membrane (Fig. 1D, E). These findings provide novel visual information indicating that although *P. gingivalis* is present to an extent even in the healthy gingival tissue, the bacterial presence is significantly higher in periodontitis tissues with distinct localization in the basal layer and near the bottom of the gingival epithelia.

Exclusive detection and localization of F. alocis *in the deep layer of the gingival epithelium in periodontitis*

Using an anti-*F. alocis* antibody with further verified specificity shown in Fig. 2A showed significantly increased levels (~ 8-fold) of *F. alocis* in the tissues from chronic periodontitis patients compared to the healthy tissue (Fig. 2B). Unlike moderately detected *P. gingivalis*, no notable staining of *F. alocis* was present in health (Fig. 2C). On the contrary, high bacterial localization was found in the periodontitis tissues, specifically in the stratum basale and lamina propria (Fig. 2D). This finding is consistent with the previous studies proposing the invasive potential of *F. alocis* (Schlafer et al., 2010). Further, we confirmed that the detected bacteria were within the tissue via three-dimensional rendering of the z-stacks from the tissues (Fig. 2E). These results for the first time visually illustrate that *F. alocis* is capable of tissue invasion with exclusive localization around/below the basal layer of the gingival epithelium in periodontitis patients.

Co-localization of P. gingivalis *and* F. alocis *specifically in periodontitis gingival tissue as well as their detection in the microvessels*

After successful examination of both *P. gingivalis* and *F. alocis* separately in gingival biopsy specimens, we performed co-immunostaining for both species on the same tissue sections to determine their comparative spatial presentations (Fig. 3A). As shown in representative micrographs of chronic periodontitis tissues, we observed highly intense co-localization of *P. gingivalis* and *F. alocis* in yellow with an average Pearson correlation coefficient of 0.88 obtained via NIH Image J software with JACoP plug-in (Fig. 3A, i-iv). While examining multiple tissue sections from all patient samples, we discovered consistent appearance of small blood vessels either specifically surrounded or invaded by both bacteria (Fig. 3A, v-viii). Further semi-quantitative analysis showed that significantly high percentage of patients in periodontitis group displayed substantially increased gingival microvasculature formation compared to that of healthy individuals (Fig. 3B).

Confirmation of gingival vasculature in periodontitis gingival epithelial tissue

To verify the gingival microvasculature we observed in multiple chronic periodontitis patient samples (Fig. 3C, i-ii), we performed

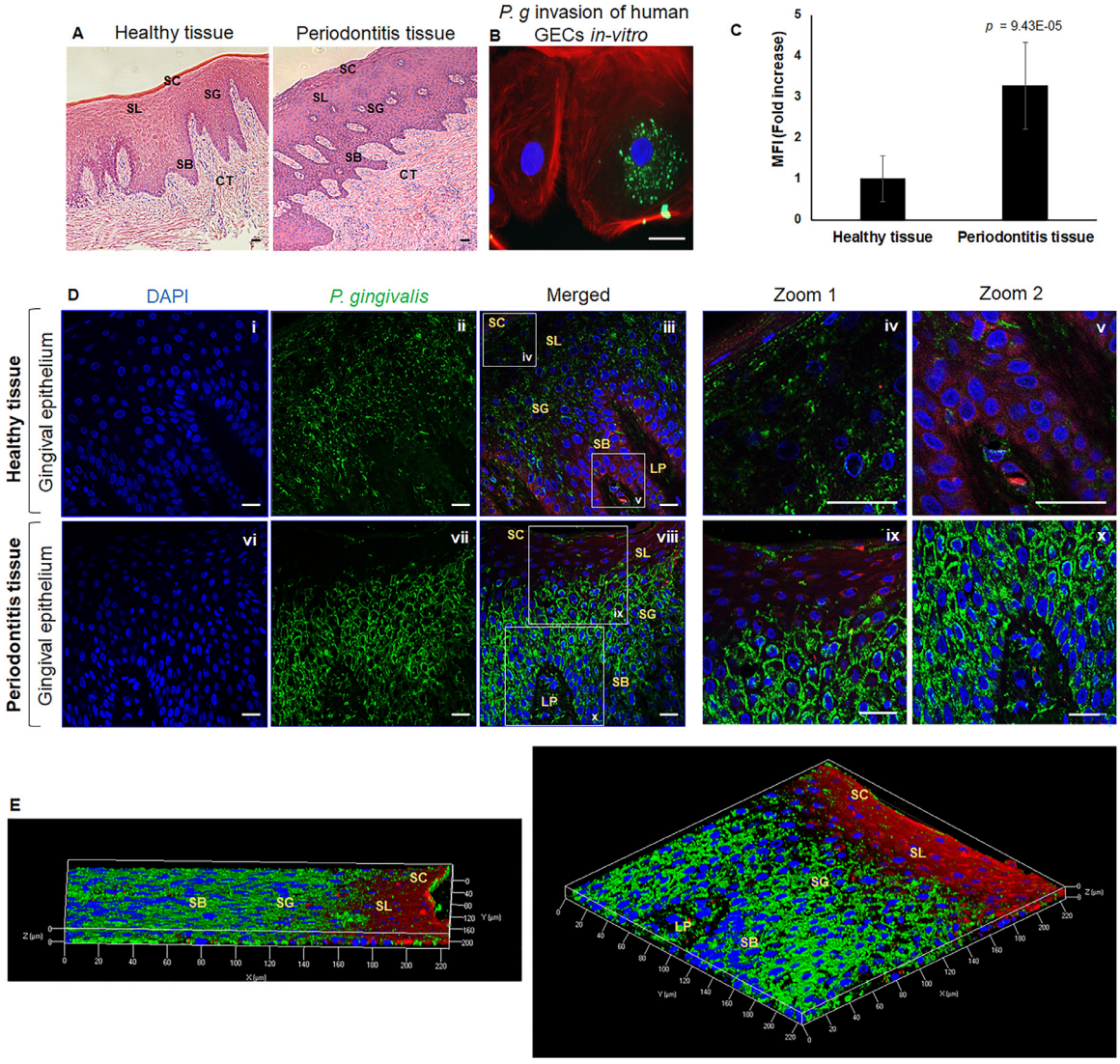

Fig. 1. Detection of *P. gingivalis* in gingival tissues in health vs. periodontitis. (A) Representative images of H&E stained gingival biopsy specimens from healthy individuals and periodontitis patients. 10x magnification. (B) The specificity of anti-*P. gingivalis* antibody is shown in the fluorescence micrograph presenting *P. gingivalis* (green) in human primary gingival epithelial cells (GECs) infected with the microorganism for 24 h. 40x magnification. (C) Mean fluorescence intensity (MFI) of *P. gingivalis* detection from gingival tissue sections in health and periodontitis obtained by confocal microscopy. Data are presented as mean ± SD. Representative images from at least 5 different patients per group were used for quantitative analysis. (D) Representative confocal images of gingival biopsy specimens from healthy individuals (i-v) and periodontitis patients (vi-x). (i, vi) 1:500 DAPI staining to visualize cellular DNA. (ii, vii) *P. gingivalis* detection using 1:200 rabbit anti-*P. gingivalis* primary antibody and 1:500 Alexafluor-488 (Green) conjugated goat anti-rabbit secondary antibody. 63x magnification with oil immersion. (iii-v, viii-x) DAPI (Blue), *P. gingivalis,* and CD73 of the gingival epithelium for a counterstaining were merged. A mouse antibody against CD73 coupled with Alexafluor-568 (Red) conjugated goat anti-mouse secondary antibody was used to outline the borders of the tissues. Images were captured using super resolution confocal laser scanning microscopy at 63x magnification with oil immersion. The range of z-stacks was kept consistent. (E) Representative three-dimensional views of z-stacks of the gingival tissue in periodontitis shown in (D; viii) to show the spatial information of the immunostained tissues. SC: Stratum corneum, SL: Stratum lucidum, SG: Stratum granulosum, SB: Stratum basale, LT: Lamina propria. Scale bars in A, B, and D = 20μm.

co-immunostaining for *P. gingivalis* and CD31, a well-established vascular marker associated with microvasculature formation (Gkontra et al., 2018) (Fig. 3C, iii-vii). The confocal micrographs demonstrated intense red fluorescence (CD31) around the structures within the epithelial layer of the tissue, suggesting the increased presence of blood vessels in the epithelium from chronic periodontitis patients (Fig. 3C, v-vii). *P. gingivalis* (green fluorescence) was also consistently localized either within or surrounding the region of the gingival microvasculature. These findings together indicate heightened formation of gingival microvasculature, which can be invaded by opportunistic pathogens such as *P. gingivalis* in periodontitis patients.

Detection of highly co-localized P. gingivalis *and* F. alocis *aggregates within the gingival microvasculature*

Our examination of tissue sections co-stained for *P. gingivalis* and *F. alocis* also revealed strong co-localization of both species within microvessels as shown in the representative confocal images (an average Pearson correlation coefficient = 0.92) (Fig. 4A, i-v), which potentially represents a novel visualization of an initial route for systemic dissemination of oral pathogens through circulation. The intense yellow signal was not a result of any unexpected cross-reactivity of the species-specific antibodies used, as there were other regions within the tissue that did

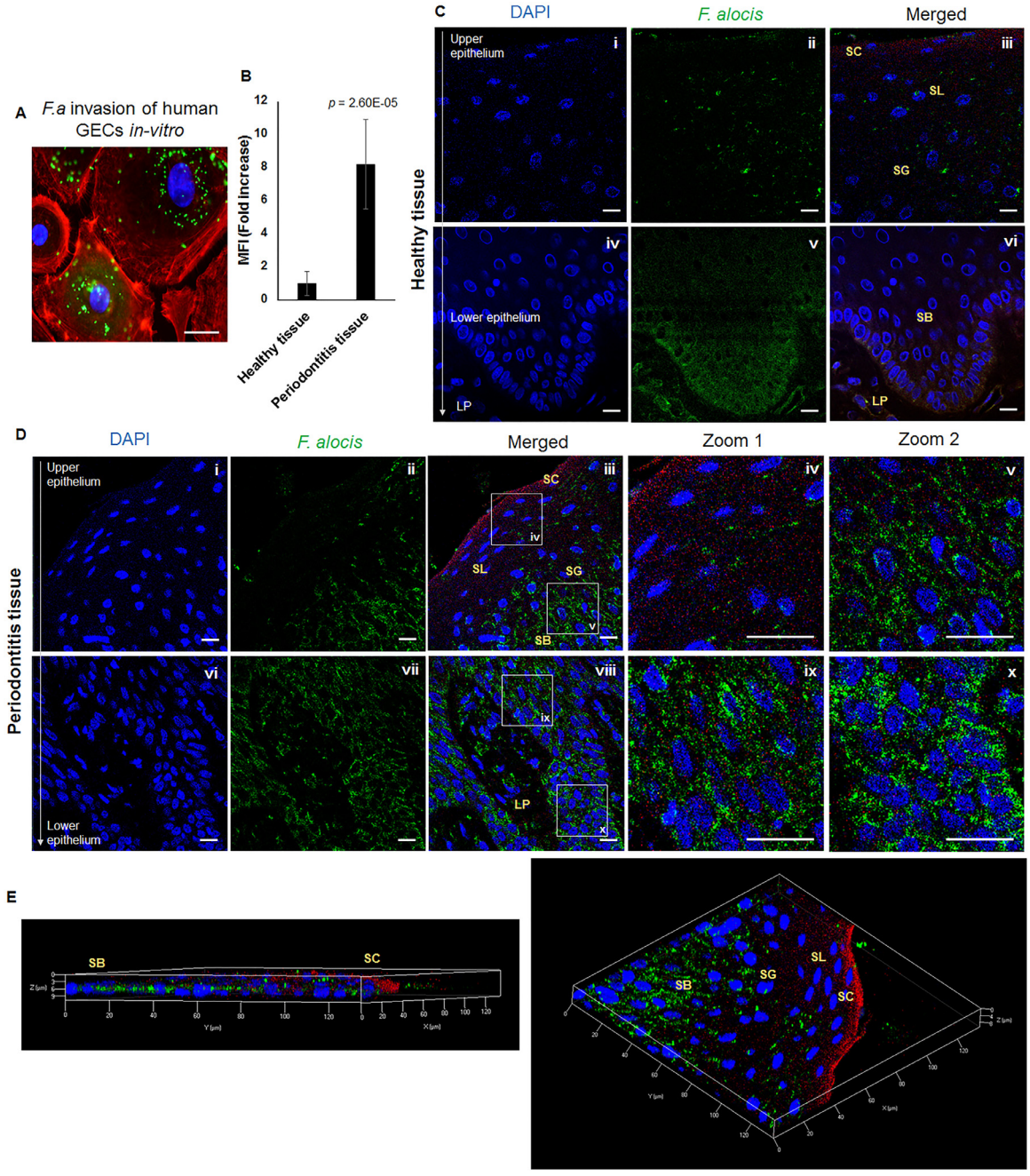

Fig. 2. Detection of *F. alocis* in gingival tissues in health vs. periodontitis. (A) The specificity of anti-*F. alocis* antibody is shown in the confocal micrograph presenting *F. alocis* (green) in human primary gingival epithelial cells (GECs) infected with the microorganism for 24 h. (B) Mean fluorescence intensity of *F. alocis* detection from gingival tissue sections in health and periodontitis obtained by confocal microscopy. Data are presented as mean ± SD. Representative images from at least 5 different patients per group were used for quantitative analysis. (C) Representative confocal images from health individuals displaying upper gingival epithelium (i-iii) and lower gingival epithelium tissue sections (iv-vi). (D) Representative confocal images from periodontitis patients displaying upper gingival epithelium (i-v) and lower gingival epithelium tissue sections (vi-x). 1:500 DAPI staining to visualize cellular DNA (C; i, iv and D; i, vi). *F. alocis* detection using 1:200 rabbit anti-*F. alocis* primary antibody and 1:500 Alexafluor-488 (Green) conjugated goat anti-rabbit secondary antibody. 63x magnification with oil emersion (C; ii, v, D; ii, vii). DAPI (Blue), *F. alocis* (Green), and CD73 of the gingival epithelium for a counterstaining were merged (C; iii, vi, D; iii-v, viii-x). A mouse antibody against CD73 coupled with Alexafluor-568 (Red) conjugated goat anti-mouse secondary antibody was used to outline the borders of the tissues. Images were captured using super resolution confocal laser scanning microscopy at 63x magnification with oil immersion. The range of z-stacks was kept consistent. (E) Representative three-dimensional views of z-stacks of the gingival tissue in periodontitis shown in (D, iii) to show the spatial information of the immunostained tissues.SC: Stratum corneum, SL: Stratum lucidum, SG: Stratum granulosum, SB: Stratum basale, LT: Lamina propria. Scale bars in A, C, and D = 20μm.

not show co-localization (Fig. 4A, vi-x). Additional controls detailed in Materials and Methods validated the antibodies. To determine an average abundance of microvessels containing *P. gingivalis* and *F. alocis* within the same tissue, we compared the number of microvessels with and without the bacteria in the gingival epithelium of each periodontitis tissue and found significantly higher percentage of microvessels within each tissue were shown to contain the bacteria (Fig. 4B). These results, therefore, suggest that *P. gingivalis* and *F. alocis* can form an aggregate within the gingival microvasculature, which perhaps creates a synergistic environment for both species and their potential dissemination into gingival vascular plexus.

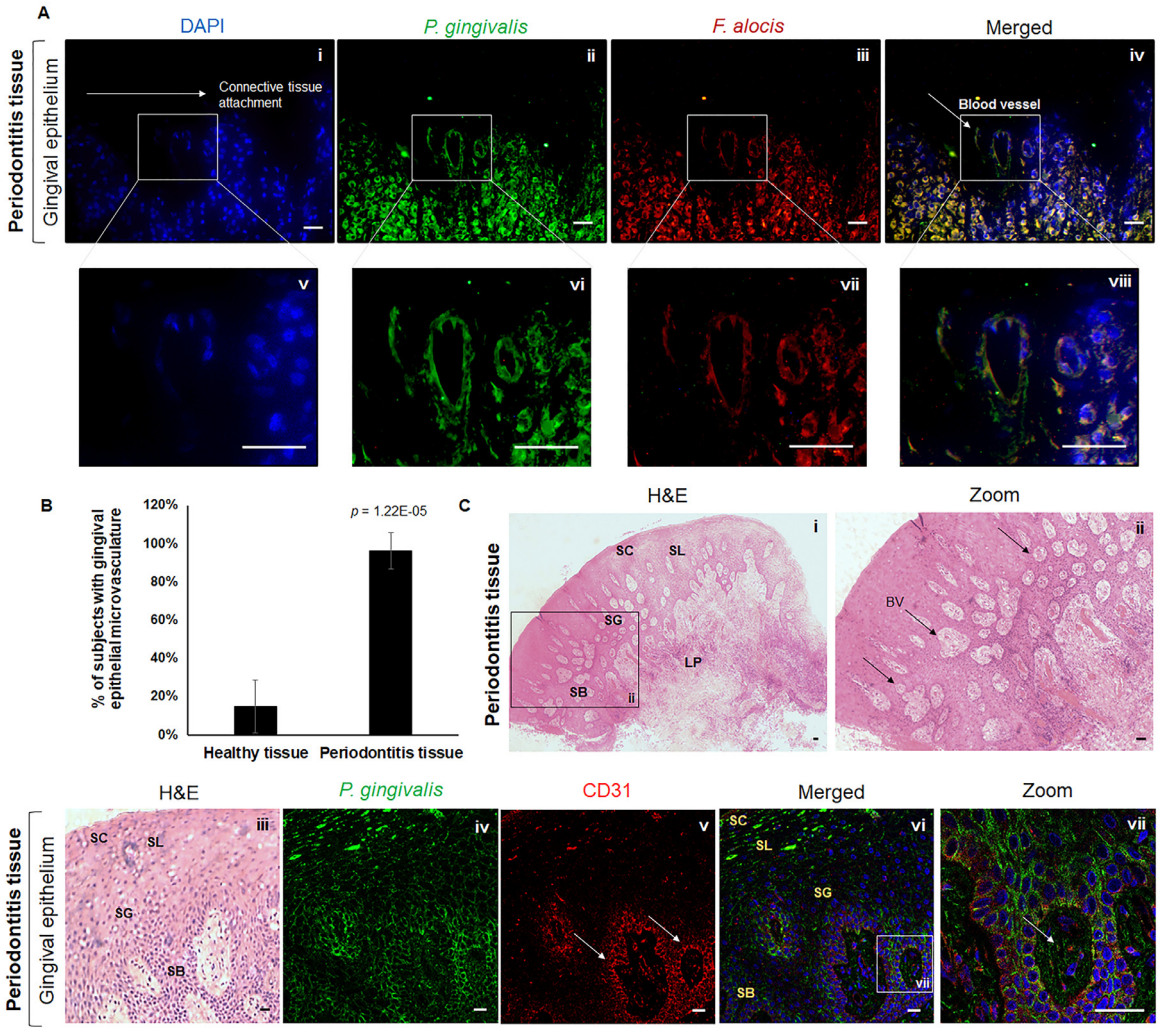

Fig. 3. Double staining of co-localized *P. gingivalis* and *F. alocis* in gingival tissue from periodontitis patients and detection of vascular structures in the epithelial layer of the periodontitis tissue. (A) Representative images of immunostained tissues from healthy individuals and periodontitis patients are shown. (i) The entrance to the sulcus on the left and connective tissue attachment on the right is with a white arrow. 1:500 DAPI staining to visualize cellular DNA. (ii) *P. gingivalis* detection using 1:200 mouse anti-*P. gingivalis* primary antibody and 1:500 Alexafluor-488 (Green) conjugated goat anti-mouse secondary antibody. (iii) *F. alocis* detection by using 1:200 rabbit anti-*F. alocis* primary antibody and 1:500 Alexafluor-568 (Red) conjugated goat anti-rabbit secondary antibody. (iv) DAPI (Blue), *P. gingivalis,* and *F. alocis* merged for co-localization with an average Pearson correlation coefficient of 0.88 via the ImageJ with JaCoP plug-in. A representative blood vessel-like structure detected is noted with a white arrow. (v-viii) Zoomed-in images highlighting a blood vessel like structure. 20x magnification. (B) The presence of microvasculature in the gingival epithelium of participants of healthy and periodontitis group in percentages. At least 3 separate sectioned slides were examined for each subject's tissue (presence or absence) and the frequency of gingival microvasculature was averaged within the group. Data are presented as mean ± SD.(C) Representative H&E stained images of gingival tissues from periodontitis patients showing heightened formation of microvasculature in the gingival epithelium. 5x (i) and 10x (ii) magnification. Black arrows indicate representative gingival microvasculature. Representative confocal microscopy images of immunostained tissue sections from gingival biopsies taken from patients diagnosed with severe chronic periodontitis. (iii) H&E staining to show tissue structure. (iv) *P. gingivalis* detection using 1:200 rabbit anti-*P. gingivalis* primary antibody and 1:500 Alexafluor-488 (Green) conjugated goat anti-rabbit secondary antibody. (v) A vascular marker CD31 antibody (mouse, monoclonal) staining followed by Alexafluor-568 (Red) conjugated goat anti-mouse secondary antibody. Arrows point to intense CD31 red staining around microvessels (vi) *P. gingivalis* (Green) and CD31 (Red) merged (vii) A zoomed-in image highlight a microvasculature in the gingival epithelium and the arrows point to high presence of *P. gingivalis* within the blood vessel. At 20x (A) and 63x (C) magnification with oil immersion. SC: Stratum corneum, SL: Stratum lucidum, SG: Stratum granulosum, SB: Stratum basale, LT: Lamina propria. Scale bars in both A and C = 20μm.

Live P. gingivalis *and* F. alocis *co-localization in human periodontitis gingival tissue*

FISH probes with *P. gingivalis* 16S rRNA-specific oligonucleotide (green) and *F. alocis* 16S rRNA-specific oligonucleotide (red) were used to identify whether the detected bacteria within the tissues were metabolically active (Fig. 5A). The results displayed strong presence of both *P. gingivalis* and *F. alocis* within the gingival epithelium (Fig. 5A, i-ix) as well as in the lamina propria of periodontitis patients (Fig. 5A, x-xiii). Whereas, in healthy biopsies, no robust fluorescence was detected in the gingival epithelium and lamina propria (data not shown). The representative micrograph of metabolically active bacteria present in the gingival epithelium also demonstrates consistent appearance of microvasculature which contains both species (Fig. 5A, iv-v, and 5B). We detected intense co-localization of *P. gingivalis* and *F. alocis* in the gingival epithelium and lamina propria (an average Pearson correlation coefficient = 0.81), which is similar with our immunostaining data. To further confirm specificity of our FISH method which already displayed specific differential detection for each species in tissues (Fig. 5A, vi-ix), we fixed cultured *P. gingivalis* ATCC 33277 or *F. alocis* ATCC 35896

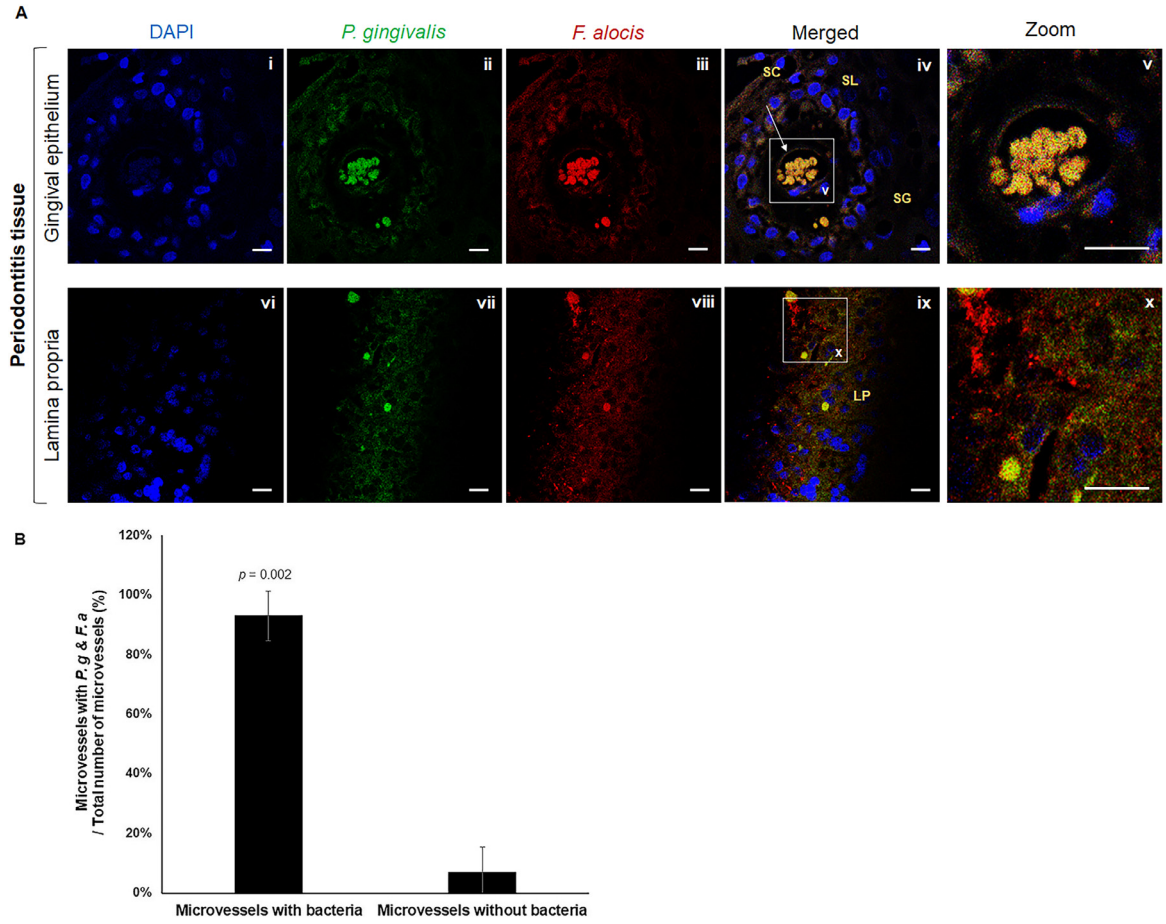

Fig. 4. Co-localization of *P. gingivalis* and *F. alocis* within the gingival microvasculature. (A) Representative confocal images of the gingival epithelium (i-v) and lamina propria (vi-x) from periodontitis patients are shown. (i, vi) 1:500 DAPI staining to visualize cellular DNA. (ii, vii) *P. gingivalis* detection using 1:200 mouse anti-*P. gingivalis* primary antibody and 1:500 Alexa Fluor 488 (Green) conjugated goat anti-mouse secondary antibody. (iii, viii) *F. alocis* detection by using 1:200 rabbit anti-*F. alocis* primary antibody and 1:500 Alexa Fluor 568 (Red) conjugated goat anti-rabbit secondary antibody. (iv, ix) DAPI (Blue), *P. gingivalis* (Green), and *F. alocis* (Red) merged. The white arrow indicates *P. gingivalis* and *F. alocis* co-localization. (v, x) Zoomed-in images highlighting co-aggregated *P. gingivalis* and *F. alocis* (yellow) invading vasculature in the gingival epithelium with an average Pearson correlation coefficient of 0.92 via the ImageJ with JaCoP plug-in. 63x magnification with oil immersion. SC: Stratum corneum, SL: Stratum lucidum, SG: Stratum granulosum, SB: Stratum basale, LT: Lamina propria. Scale bars = 20μm. (B) The number of microvessels with and without both bacteria out of all microvessels present within the same tissue in percentages. Each periodontitis tissue presenting robust gingival microvasculature was examined. The number of microvessels with the bacteria, without the bacteria, and total number of vessels present were recorded for quantification. Data are presented as mean ± SD.

on microscopic slides and hybridized each bacteria with either P.g-488 FISH or F.a-594 probe individually which also validated the specificity of FISH method (Supplemental Fig. 1). These results collectively revealed strong dual occurrence of *P. gingivalis* and *F. alocis* in an active state within the epithelial tissue from periodontitis patients.

Discussion

This study unraveled a novel interaction between *P. gingivalis* and *F. alocis* in human periodontal gingiva, including the co-invasion of these two bacteria deep epithelial layers, lamina propria, and the gingival epithelial microvasculature from periodontitis patients. Our *in situ* comparative analysis suggested a substantial difference in the *P. gingivalis* levels in health vs. periodontitis, while a moderate amount of *P. gingivalis* was present in healthy gingival tissue. This finding is consistent with existing studies that reported elevated *P. gingivalis* levels in periodontitis patients compared to those in healthy individuals (Colombo et al., 2009, Colombo et al., 2007, Rudney and Chen, 2006). Across our patient samples, most of *P. gingivalis* in healthy tissue appears to be contained within the gingival epithelium, whereas a widespread distribution of the bacteria past the epithelial layer was observed in periodontitis. On the contrary, only indiscernible levels of *F. alocis* were detected in the gingival epithelium and in the lamina propria from healthy individuals. In periodontitis tissues, highly detectable levels of *F. alocis* were intensely concentrated within the lamina propria showing ability of *F. alocis* as a deeper tissue invading pathogen. This finding is also consistent with the previous studies that have suggested *F. alocis* as a marker for periodontitis (Kumar et al., 2006).

Although potential physical interactions of both species have been previously suggested (Wang et al., 2013), the inter-species connection between *P. gingivalis* and *F. alocis* have been mainly limited to biofilm-based *in vitro* community development models. To date, there is no substantial evidence that directly shows the presence of the two species within human gingival tissues, which is considered the most clinically relevant way of understanding the distribution of the pathogens. In our study, we examined the differential localization of *P. gingivalis* and *F. alocis* together by species specific immunostaining human gingival tissues in health and periodontitis and demonstrated the organismal viability via the 16S rRNA specific FISH method. Despite the assumed differences in detection sensitivities of fluorescence signals between the use

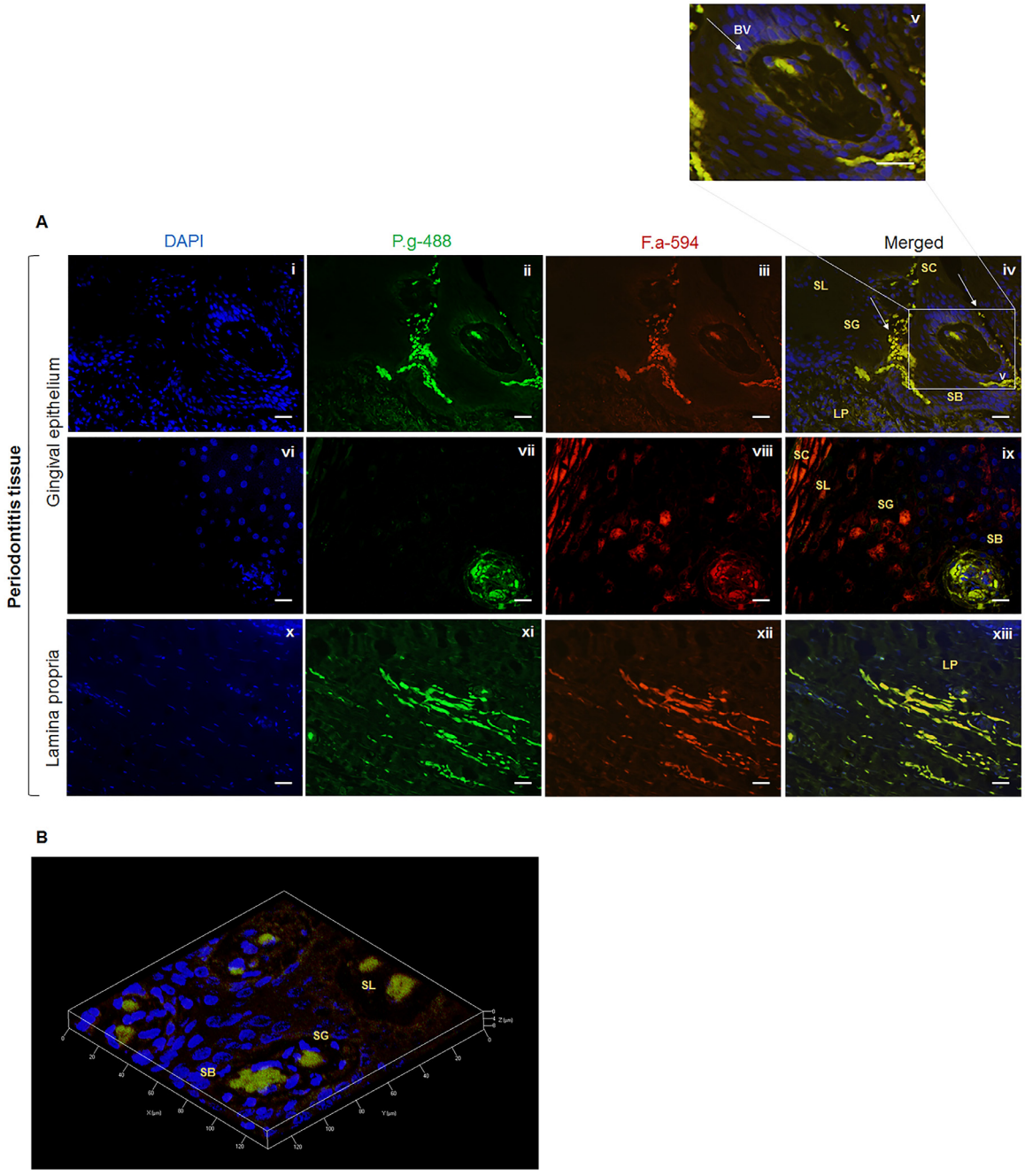

Fig. 5. Co-colonization of metabolically active *P. gingivalis* and *F. alocis* within the gingival tissue in periodontitis. (A) Representative micrographs of live *P. gingivalis* and *F. alocis* within the epithelial layer (i-ix) and lamina propria (x-xiii) of gingiva sections from patients with chronic periodontitis via FISH method as previously described (Velsko et al., 2014, Schlafer et al., 2010). Hybridization was performed using *P. gingivalis* 16S rRNA-specific oligonucleotide POGI labeled with Alexafluor 488 (Green fluorescent) and *F. alocis* 16S rRNA-specific oligonucleotide FIAL labeled with Alexafluor-594 (Red fluorescent) probes. (i, vi, x) 1:500 DAPI (Blue) staining to visualize cellular DNA. (ii, vii, xi) Metabolically active *P. gingivalis* detection using 5nM *P. gingivalis* specific probe tagged with Alexafluor-488. (iii, viii, xiii) Metabolically active *F. alocis* detection using 5nM *F.a* specific probe tagged with Alexafluor-594. (iv, ix, xiii) DAPI, *P. gingivalis, F. alocis* merged. The white arrows indicate both bacterial species are invading deeper into the tissue in mixed colonies through the epithelial tissue. Co-localization of the two species is shown in yellow with an average Pearson correlation coefficient of 0.90 via the ImageJ with JaCoP plug-in. (v) Co-localization of live *P. gingivalis* and *F. alocis* is also detected in a blood vessel (BV) as denoted with a white arrow. Images were obtained with 20x magnification on Zeiss Axio Imager. SC: Stratum corneum, SL: Stratum lucidum, SG: Stratum granulosum, SB: Stratum basale, LT: Lamina propria. Scale bars = 20μm. (B) A representative three-dimensional view of gingival tissue in periodontitis stained with FISH probes for *P. gingivalis* and *F. alocis* to display the spatial information.

of antibodies and FISH probes, our results for *P. gingivalis* and *F. alocis* using both methods suggest that the two organisms, in a metabolically active state, are co-localized within the periodontitis tissue in specific locations.

Currently, the only published clinical study involves fluorescence *in situ* hybridization examination of *F. alocis* is in the context of biofilm structure (Schlafer et al., 2010). Similarly, there are limited reports of *P. gingivalis* observed in patient tissues (Saglie et al., 1982, Baek et al., 2018, Katz et al., 2011, Choi et al., 2014, Carranza et al., 1983). Recent reports claim that normal physiological architecture of gingival tissues can be disorganized by oral pathogens including *P. gingivalis* and microorganisms may possess the capability to form complex polymicro-

bial structures directly within the tissues (Baek et al., 2018, Choi et al., 2014). Interestingly, we present here a novel association of *P. gingivalis* and *F. alocis* within the periodontal tissues. It seems reasonable to propose that *P. gingivalis* may partner with *F. alocis*, to establish chronic niduses of infection in gingival epithelium and underlying periodontal tissue. This notion is agreeing with the recently discovered line of evidence for *P. gingivalis* in human primary gingival epithelial cells showing the formation of double-membrane autophagic structures as replicative intracellular niches for the survival of this well-adapted pathogen (Lee et al., 2018) before *P. gingivalis* can spread intercellularly within gingiva (Yilmaz et al., 2006).

Our findings also illustrated that gingival tissues from periodontitis patients reveal increased formation of gingival microvasculature. The microvasculature formation within the gingival epithelium is consistent with chronic inflammation and the clinical sign of bleeding on probing (Prakash et al., 2014). However, there has been no robust evidence indicating the localization of periodontal pathogens, such as *P. gingivalis* and *F. alocis* within the microvessels. Here, our study shows not only the congruent finding of gingival microvasculature in periodontitis, but also depicting prevalently co-localized active aggregate of *P. gingivalis* and *F. alocis* within those vessels. In addition to the mucosal invasion associated with the presence of the microorganisms, this observation further demonstrates a newly recognized direct path of periodontal bacterial dissemination in host.

In conclusion, *P. gingivalis* and *F. alocis* may establish joint colonization niches in gingival epithelia to build a complex reservoir structure against host immune defenses and to increase their survival in oral mucosa, which could eventually lead to microbial dysbiosis and systemic bacterial spread. However, our findings may be restricted to our patient population in this present study. Therefore, despite the agreement with the previous literature in some respects, it might be early for the novel findings of our study to be largely generalized. Further systems level comprehensive studies will be needed to help answer these complex questions.

Declaration of Competing Interest

The authors declare that they have no known competing financial interests or personal relationships that could have appeared to influence the work reported in this paper.

Acknowledgements

The authors would like to thank Dr. Brad Neville, DMD, Diplomate Oral Pathologist and Mrs. Sue Newton for their invaluable expertise and help with processing of tissue specimens and interpreting them; Dr. Michael Cuenin, DMD, Periodontics Program Director for his critical guidance on this project. This work was supported by funding from the NIH grants R01DE016593, R56DE016593, T32DE017551, F30DE029103 and UL1TR001450.

The views expressed in this article are those of the author(s) and do not necessarily reflect the official policy or position of the Department of the Navy, Department of Defense, or the United States Government. “Author, Dr. Ralee Spooner is a military service member (or employee of the U.S. Government). This work was prepared as part of his official duties.” Title 17, USC, §105 provides that ‘Copyright protection under this title is not available for any work of the U.S. Government. Title 17, USC, §101 defines a U.S. Government work as a work prepared by a military service member or employee of the U.S. Government as part of that person’s official duties.

Supplementary materials

Supplementary material associated with this article can be found, in the online version, at doi:10.1016/j.crmicr.2020.05.001.

References

American Academy of Periodontology Task Force, 2015. Report on the Update to the 1999 Classification of Periodontal Diseases and Conditions. J Periodontol 86, 835–838.

Aruni, A.W., Roy, F., Fletcher, H.M., 2011. *Filifactor alocis* has virulence attributes that can enhance its persistence under oxidative stress conditions and mediate invasion of epithelial cells by *Porphyromonas gingivalis*. Infect Immun 79, 3872–3886.

Atanasova, K., Lee, J., Roberts, J., Lee, K., Ojcius, D.M., Yilmaz, Ö., 2016. Nucleoside-Diphosphate-Kinase of *P. gingivalis* is Secreted from Epithelial Cells In the Absence of a Leader Sequence Through a Pannexin-1 Interactome. Scientific reports 6, 37643.

Atanasova, K.R., Yilmaz, O., 2014. Looking in the *Porphyromonas gingivalis* cabinet of curiosities: the microbium, the host and cancer association. Mol Oral Microbiol 29, 55–66.

Atanasova, K.R., Yilmaz, O., 2015. Prelude to oral microbes and chronic diseases: past, present and future. Microbes Infect 17, 473–483.

Azaripour, A., Lagerweij, T., Scharfbillig, C., Jadczak, A.E., Swaan, B.V., Molenaar, M., Waal, R.V., Kielbassa, K., Tigchelaar, W., Picavet, D.I., et al., 2018. Three-dimensional histochemistry and imaging of human gingiva. Sci Rep 8, 1647.

Baek, K., Ji, S., Choi, Y., 2018. Complex Intratissue Microbiota Forms Biofilms in Periodontal Lesions. J Dent Res 97, 192–200.

Bale, B.F., Doneen, A.L., Vigerust, D.J., 2017. High-risk periodontal pathogens contribute to the pathogenesis of atherosclerosis. Postgrad Med J 93, 215–220.

Bolte, S., Cordelieres, F.P., 2006. A guided tour into subcellular colocalization analysis in light microscopy. J Microsc 224, 213–232.

Bui, F.Q., Johnson, L., Roberts, J., Hung, S.C., Lee, J., Atanasova, K.R., Huang, P.R., Yilmaz, O., Ojcius, D.M., 2016. *Fusobacterium nucleatum* infection of gingival epithelial cells leads to NLRP3 inflammasome-dependent secretion of IL-1beta and the danger signals ASC and HMGB1. Cell Microbiol 18, 970–981.

Carranza Jr., F.A., Saglie, R., Newman, M.G., Valentin, P.L., 1983. Scanning and transmission electron microscopic study of tissue-invading microorganisms in localized juvenile periodontitis. J Periodontol 54, 598–617.

Chen, H., Liu, Y., Zhang, M., Wang, G., Qi, Z., Bridgewater, L., Zhao, L., Tang, Z., Pang, X., 2015. A *Filifactor alocis*-centered co-occurrence group associates with periodontitis across different oral habitats. Sci Rep 5, 9053.

Choi, C.H., DeGuzman, J.V., Lamont, R.J., Yilmaz, O., 2011. Genetic transformation of an obligate anaerobe, *P. gingivalis* for FMN-green fluorescent protein expression in studying host-microbe interaction. PLoS One 6, e18499.

Choi, C.H., Spooner, R., DeGuzman, J., Koutouzis, T., Ojcius, D.M., Yilmaz, Ö., 2013. *Porphyromonas gingivalis*-nucleoside-diphosphate-kinase inhibits ATP-induced reactive-oxygen-species via P2X7 receptor/NADPH-oxidase signalling and contributes to persistence. Cellular microbiology 15, 961–976.

Choi, Y.S., Kim, Y.C., Ji, S., Choi, Y., 2014. Increased bacterial invasion and differential expression of tight-junction proteins, growth factors, and growth factor receptors in periodontal lesions. J Periodontol 85, e313–e322.

Colombo, A.P., Bennet, S., Cotton, S.L., Goodson, J.M., Kent, R., Haffajee, A.D., Socransky, S.S., Hasturk, H., Van Dyke, T.E., Dewhirst, F.E., et al., 2012. Impact of periodontal therapy on the subgingival microbiota of severe periodontitis: comparison between good responders and individuals with refractory periodontitis using the human oral microbe identification microarray. J Periodontol 83, 1279–1287.

Colombo, A.P., Boches, S.K., Cotton, S.L., Goodson, J.M., Kent, R., Haffajee, A.D., Socransky, S.S., Hasturk, H., Van Dyke, T.E., Dewhirst, F., et al., 2009. Comparisons of subgingival microbial profiles of refractory periodontitis, severe periodontitis, and periodontal health using the human oral microbe identification microarray. J Periodontol 80, 1421–1432.

Colombo, A.V., da Silva, C.M., Haffajee, A., Colombo, A.P., 2007. Identification of intracellular oral species within human crevicular epithelial cells from subjects with chronic periodontitis by fluorescence in situ hybridization. J Periodontal Res 42, 236–243.

Dewhirst, F.E., Chen, T., Izard, J., Paster, B.J., Tanner, A.C., Yu, W.H., Lakshmanan, A., Wade, W.G., 2010. The human oral microbiome. J Bacteriol 192, 5002–5017.

Dominy, S.S., Lynch, C., Ermini, F., Benedyk, M., Marczyk, A., Konradi, A., Nguyen, M., Haditsch, U., Raha, D., Griffin, C., et al., 2019. *Porphyromonas gingivalis* in Alzheimer’s disease brains: Evidence for disease causation and treatment with small-molecule inhibitors. Sci Adv 5, eaau3333.

Dunn, K.W., Kamocka, M.M., McDonald, J.H., 2011. A practical guide to evaluating colocalization in biological microscopy. Am J Physiol Cell Physiol 300, C723–C742.

Gkontra, P., Norton, K.A., Zak, M.M., Clemente, C., Aguero, J., Ibanez, B., Santos, A., Popel, A.S., Arroyo, A.G., 2018. Deciphering microvascular changes after myocardial infarction through 3D fully automated image analysis. Sci Rep 8, 1854.

Hajishengallis, G., Darveau, R.P., Curtis, M.A., 2012. The keystone-pathogen hypothesis. Nat Rev Microbiol 10, 717–725.

Hung, S.C., Choi, C.H., Said-Sadier, N., Johnson, L., Atanasova, K.R., Sellami, H., Yilmaz, O., Ojcius, D.M., 2013. P2X4 assembles with P2X7 and pannexin-1 in gingival epithelial cells and modulates ATP-induced reactive oxygen species production and inflammasome activation. PLoS One 8, e70210.

Ji, S., Choi, Y.S., Choi, Y., 2015. Bacterial invasion and persistence: critical events in the pathogenesis of periodontitis? J Periodontal Res 50, 570–585.

Junemann, S., Prior, K., Szczepanowski, R., Harks, I., Ehmke, B., Goesmann, A., Stoye, J., Harmsen, D., 2012. Bacterial community shift in treated periodontitis patients revealed by ion torrent 16S rRNA gene amplicon sequencing. PLoS One 7, e41606.

Katz, J., Onate, M.D., Pauley, K.M., Bhattacharyya, I., Cha, S., 2011. Presence of *Porphyromonas gingivalis* in gingival squamous cell carcinoma. Int J Oral Sci 3, 209–215.

Kumar, P.S., Leys, E.J., Bryk, J.M., Martinez, F.J., Moeschberger, M.L., Griffen, A.L., 2006. Changes in periodontal health status are associated with bacterial community shifts as assessed by quantitative 16S cloning and sequencing. J Clin Microbiol 44, 3665–3673.

Lamont, R.J., Chan, A., Belton, C.M., Izutsu, K.T., Vasel, D., Weinberg, A., 1995. *Porphyromonas gingivalis* invasion of gingival epithelial cells. Infect Immun 63, 3878–3885.
Lamont, R.J., Koo, H., Hajishengallis, G., 2018. The oral microbiota: dynamic communities and host interactions. Nat Rev Microbiol 16, 745–759.
Lee, J., Roberts, J.S., Atanasova, K.R., Chowdhury, N., Han, K., Yilmaz, O., 2017. Human Primary Epithelial Cells Acquire an Epithelial-Mesenchymal-Transition Phenotype during Long-Term Infection by the Oral Opportunistic Pathogen, *Porphyromonas gingivalis*. Front Cell Infect Microbiol 7, 493.
Lee, J., Roberts, J.S., Atanasova, K.R., Chowdhury, N., Yilmaz, O., 2018. A novel kinase function of a nucleoside-diphosphate-kinase homologue in *Porphyromonas gingivalis* is critical in subversion of host cell apoptosis by targeting heat-shock protein 27. Cell Microbiol 20, e12825.
Lee, J.S., Chowdhury, N., Roberts, J.S., Yilmaz, O., 2020. Host surface ectonucleotidase-CD73 and the opportunistic pathogen, *Porphyromonas gingivalis*, cross-modulation underlies a new homeostatic mechanism for chronic bacterial survival in human epithelial cells. Virulence 11 414–429.
Lee, K., Roberts, J.S., Choi, C.H., Atanasova, K.R., Yilmaz, O., 2018. *Porphyromonas gingivalis* traffics into endoplasmic reticulum-rich-autophagosomes for successful survival in human gingival epithelial cells. Virulence 9, 845–859.
Olsen, I., Yilmaz, O., 2019. Possible role of *Porphyromonas gingivalis* in orodigestive cancers. J Oral Microbiol 11, 1563410.
Pihlstrom, B.L., Michalowicz, B.S., Johnson, N.W., 2005. Periodontal diseases. Lancet 366, 1809–1820.
Prakash, P., Rath, S., Mukherjee, M., Malik, A., Boruah, D., Sahoo, N.K., Dutta, V., 2014. Comparative evaluation of the marginal gingival epithelium in smokers and nonsmokers: a histomorphometric and immunohistochemical study. Int J Periodontics Restorative Dent 34, 781–786.
Rajakaruna, G.A., Negi, M., Uchida, K., Sekine, M., Furukawa, A., Ito, T., Kobayashi, D., Suzuki, Y., Akashi, T., Umeda, M., et al., 2018. Localization and density of *Porphyromonas gingivalis* and *Tannerella forsythia* in gingival and subgingival granulation tissues affected by chronic or aggressive periodontitis. Sci Rep 8, 9507.
Roberts, J.S., Atanasova, K.R., Lee, J., Diamond, G., Deguzman, J., Hee Choi, C., Yilmaz, Ö., 2017. Opportunistic Pathogen *Porphyromonas gingivalis* Modulates Danger Signal ATP-Mediated Antibacterial NOX2 Pathways in Primary Epithelial Cells. Frontiers in Cellular and Infection Microbiology 7, 291.
Rudney, J.D., Chen, R., 2006. The vital status of human buccal epithelial cells and the bacteria associated with them. Arch Oral Biol 51, 291–298.
Saglie, R., Newman, M.G., Carranza Jr., F.A., Pattison, G.L., 1982. Bacterial invasion of gingiva in advanced periodontitis in humans. J Periodontol 53, 217–222.
Schlafer, S., Riep, B., Griffen, A.L., Petrich, A., Hubner, J., Berning, M., Friedmann, A., Gobel, U.B., Moter, A., 2010. *Filifactor alocis*–involvement in periodontal biofilms. BMC Microbiol 10, 66.
Socransky, S.S., Haffajee, A.D., 1992. The bacterial etiology of destructive periodontal disease: current concepts. Journal of periodontology 63, 322–331.
Socransky, S.S., Haffajee, A.D., 2005. Periodontal microbial ecology. Periodontol 2000 38, 135–187.
Socransky, S.S., Haffajee, A.D., Cugini, M.A., Smith, C., Kent Jr., R.L., 1998. Microbial complexes in subgingival plaque. J Clin Periodontol 25, 134–144.
Spooner, R., DeGuzman, J., Lee, K.L., Yilmaz, O., 2014. Danger signal adenosine via adenosine 2a receptor stimulates growth of *Porphyromonas gingivalis* in primary gingival epithelial cells. Molecular oral microbiology 29, 67–78.
Spooner, R., Weigel, K.M., Harrison, P.L., Lee, K., Cangelosi, G.A., Yilmaz, O., 2016. In Situ Anabolic Activity of Periodontal Pathogens *Porphyromonas gingivalis* and *Filifactor alocis* in Chronic Periodontitis. Sci Rep 6, 33638.
Sunde, P.T., Olsen, I., Gobel, U.B., Theegarten, D., Winter, S., Debelian, G.J., Tronstad, L., Moter, A., 2003. Fluorescence in situ hybridization (FISH) for direct visualization of bacteria in periapical lesions of asymptomatic root-filled teeth. Microbiology 149, 1095–1102.
Velsko, I.M., Chukkapalli, S.S., Rivera, M.F., Lee, J.Y., Chen, H., Zheng, D., Bhattacharyya, I., Gangula, P.R., Lucas, A.R., Kesavalu, L., 2014. Active invasion of oral and aortic tissues by *Porphyromonas gingivalis* in mice causally links periodontitis and atherosclerosis. PLoS One 9, e97811.
Wang, Q., Wright, C.J., Dingming, H., Uriarte, S.M., Lamont, R.J., 2013. Oral community interactions of *Filifactor alocis* in vitro. PLoS One 8, e76271.
Yang, H.W., Huang, Y.F., Chou, M.Y., 2004. Occurrence of *Porphyromonas gingivalis* and Tannerella forsythensis in periodontally diseased and healthy subjects. J Periodontol 75, 1077–1083.
Yilmaz, O., 2008. The chronicles of *Porphyromonas gingivalis*: the microbium, the human oral epithelium and their interplay. Microbiology 154, 2897–2903.
Yilmaz, O., Jungas, T., Verbeke, P., Ojcius, D.M., 2004. Activation of the phosphatidylinositol 3-kinase/Akt pathway contributes to survival of primary epithelial cells infected with the periodontal pathogen *Porphyromonas gingivalis*. Infection and immunity 72, 3743–3751.
Yilmaz, O., Verbeke, P., Lamont, R.J., Ojcius, D.M., 2006. Intercellular spreading of *Porphyromonas gingivalis* infection in primary gingival epithelial cells. Infect Immun 74, 703–710.
Yilmaz, O., Yao, L., Maeda, K., Rose, T.M., Lewis, E.L., Duman, M., Lamont, R.J., Ojcius, D.M., 2008. ATP scavenging by the intracellular pathogen *Porphyromonas gingivalis* inhibits P2X7-mediated host-cell apoptosis. Cell Microbiol 10, 863–875.
Yilmaz, O., Young, P.A., Lamont, R.J., Kenny, G.E., 2003. Gingival epithelial cell signalling and cytoskeletal responses to *Porphyromonas gingivalis* invasion. Microbiology 149, 2417–2426.
Yu, Q.C., Song, W., Wang, D., Zeng, Y.A., 2016. Identification of blood vascular endothelial stem cells by the expression of protein C receptor. Cell Res 26, 1079–1098.
Zhang, S., Hu, L., Jiang, J., Li, H., Wu, Q., Ooi, K., Wang, J., Feng, Y., Zhu, D., Xia, C., 2020. HMGB1/RAGE axis mediates stress-induced RVLM neuroinflammation in mice via impairing mitophagy flux in microglia. J Neuroinflammation 17, 15.